Fermi National Accelerator Laboratory

FERMILAB-Conf-79/86-EXP
7410.594

THE CONSTRUCTION AND PERFORMANCE OF LARGE FLASH CHAMBERS

F. E. Taylor, D. Bogert, R. Fisk, L. Stutte,
J. K. Walker, and J. Wolfson
Fermi National Accelerator Laboratory, Batavia, Illinois 60510

and

M. Abolins, J. Ernwein, and D. Owen
Michigan State University, East Lansing, Michigan 48824

and

T. Lyons
Massachusetts Institute of Technology, Cambridge, Massachusetts 02139

December 1979

(Presented at the IEEE Nuclear Science Symposium, San Francisco, California, October 17-19, 1979)

THE CONSTRUCTION AND PERFORMANCE OF LARGE FLASH CHAMBERS

F.E. Taylor*, D. Bogert, R.Fisk,
L.Stutte, J.K.Walker, and J.Wolfson,
Fermi National Accelerator Laboratory
and
M. Abolins, J. Ernwein, and D.Owen,
Michigan State University
and
T. Lyons
Massachusetts Institute of Technology

Abstract

The constuction and performance of 12' x 12' flash chambers used in a 340 ton neutrino detector under construction at Fermilab is described. The flash chambers supply digital information with a spatial resolution of 0.2", and are used to finely sample the shower development of the reaction products of neutrino interactions. The flash chambers are easy and inexpensive to build and are electronically read out.

Introduction

The central problem in building a neutrino detector is to instrument a large mass with a fine grain sampling of the final state shower to achieve good spatial resolution and a high pattern recognition capability. Several techniques have been recently developed which address this problem. Each technique is a different compromise of cost, spatial resolution, shower sampling step and technological complexity. The flash chamber is a simple, "low technology" instrument which achieves good spatial resolution. Because of its low cost, the flash chamber may be used to make a fine grain calorimeter with excellent pattern recognition capability and good energy and angle resolution. Hence the flash chamber is a good instrument to employ in a large neutrino detector.

Recently Conversi and coworkers[1] have developed a simple and inexpensive method of constructing flash chambers. A sheet of polypropylene plastic extruded in a honeycomb shape with 0.20" x 0.23" (5.0 mm x 5.8 mm) rectangular cells is fitted with gas manifolds which allows a pure Ne-He gas mixture to be maintained inside the cells. High voltage electrodes are glued to both sides of the polypropylene sheet. When a charged particle of interest traverses the polypropylene sheet, the high voltage electric field is applied thereby creating a plasma discharge in the cell which had been traversed by the particle. This plasma discharge propagates down the full length of the flash chamber to a region near the gas manifolds where it may be read out electronically or optically.

This report will describe the construction and performance of 12' x 12' (3.7 m x 3.7 m flash chambers which are being built for the FMMN (Fermilab-MIT-MSU-NIU) collaboration at FNAL. The low cost and simplicity of the flash chamber has made it feasible to construct a large 340 metric ton calorimeter consisting of more than 600 flash chamber planes. This allows a find grained sampling (3.61 g/cm^2) of the showers from high energy neutrino interactions. The calorimeter is presently under construction and will for the first experiments be used to study ν_μ nucleon deep inelastic scattering via the weak neutral current in the narrow band beam and ν_μ-e elastic scattering in the wide band beam.

Construction of Flash Chambers

The flash chambers are built in 3 different views X, Y and U, which have cells 0°, 80°, and 100° respectively with respect to the horizontal plane. Each chamber is constructed from three 4' (1.22 m) wide black polypropylene sheets to form a total chamber sensitive area of 12' x 12' corresponding to roughly 635 cells. The three polypropylene sheets are fastened together by mylar tape to prevent sparking through the seams between polypropylene sheets. Aluminum foils, 5 mils thick and 36" wide by 14' long are glued with a water base latex contact glue to the polypropylene to form the HV electrodes. The aluminum foils are overlapped by 3" and are fastened together by conductive aluminum tape. The HV electrodes are cut back 12" from the gas manifolds to quench the plasma discharge before it reaches the gas manifolds thereby eliminating cell-to-cell cross talk.

The gas manifolds are made by welding translucent polypropylene strips around the ends of each 4' wide polypropylene sheet. The ends of the translucent polypropylene are fused together by heat to complete the gas seal. A polypropylene tube with 40 mil diameter holes every 2" along its length is inserted in each gas manifold to evenly distribute the gas within the polypropylene sheet.

The use of a welded polypropylene construction avoids the outgassing and uncertain strength of adhesive bonding to polypropylene and thus circumvents a major construction difficulty. We have refined this sealing method so that is is very rapid to execute, and produces a reliable gas seal.

Standard 90% Ne-10% He gas with no quenchers is used in the chambers. The gas flows from the read out region through the chambers at a rate of 1.5% chambers volume/min. and is continuously purified and recirculated by a two sieve gas purification system.

Fig. 1 shows the construction of an X chamber. (The Y and U chamber construction is quite similar.) The chambers can be constructed by unskilled labor using a knife, soldering gun, plastic welders, glue and tape.

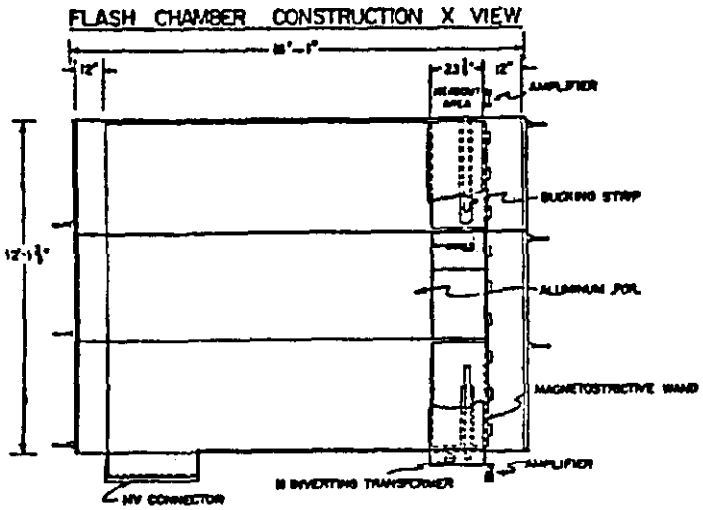

Fig. 1 Construction of an X chamber.

The High Voltage Pulsing System

To achieve good efficiency independent of location on the chambers, the high voltage pulse must have a rise time 10% to 90% full amplitude of ~ 30 nsec over the entire chamber area and have a duration of approximately 500 nsec at a voltage of 5 kV. The HV rise time is critical in initiating the plasma discharge. Measurements indicate that the chamber efficiency is degraded by 14% if the high voltage pulse rise time is increased from 40 nanoseconds to 100 nanoseconds. The duration of the HV pulse is critical in sustaining the plasma discharge long enough for it to propagate down the cell to the readout section. The plasma propagates down the polypropylene cell at a speed which depends slowly on the high voltage. For 5 kV across the polypropylene the progation speed is roughly 10 nanoseconds/foot.

Figure 2a shows the linear distance versus time relation for plasma propagation generated by a square high voltage pulse. Figure 2b shows the more complex distance-time relation for the actual high voltage pulse used on the flash chambers. The higher propagation speed at the onset of the discharge corresponds to the fast spike at the beginning of the high voltage pulse.

The HV pulse is produced by a pulse forming network (PFN) of a characteristic impedence of 5 Ω. Each chamber is equipped with its own PFN. A triggered spark gap, which employes a spark plug (Champion L-20 V), acts as the switching element of the PFN. The spark gap is operated in dry N_2 gas at atmospheric pressure.

The capacitance of the PFN is distributed in 3 locations with more capacitance in the first stage to insure good rise time. Figure 3 shows the PFN circuit. The capacitors for the first stage of the PFN are six of the standard "door knob" type rated at 15 kV -6.5 nf. These are mounted in parallel. The middle and last stages employ 30 nf mica capacitors. The inductors are small coils of ignition cable and have L ≃ 0.4 μh. The 3.3 Ω resistance in series with the second inductor damps the after ringing of the HV pulse. The flash chamber capacitance is roughly 30 nanofarads. A typical HV pulse is shown in Fig. 3.

The HV pulse is fed into the chamber by a 30" wide HV tongue at one corner of the chamber and is terminated with two-10 Ω/2 watt carbon resistors in parallel on the opposite side of the chamber. No significant variations of the high voltage pulse shape is observed at different locations on the chamber.

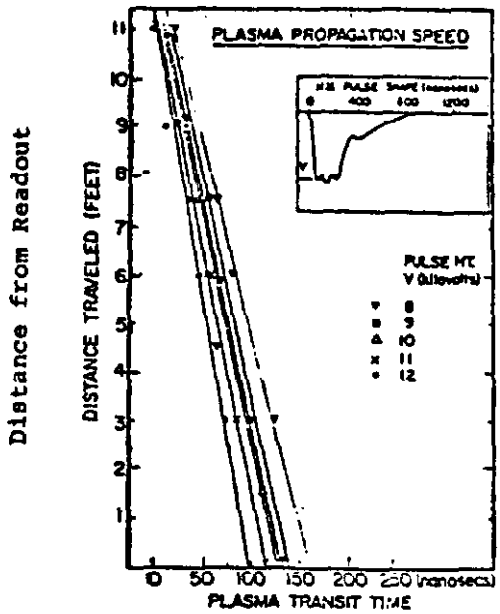

Fig. 2a Distance vs. time of the plasma propagation fo square HV pulse.

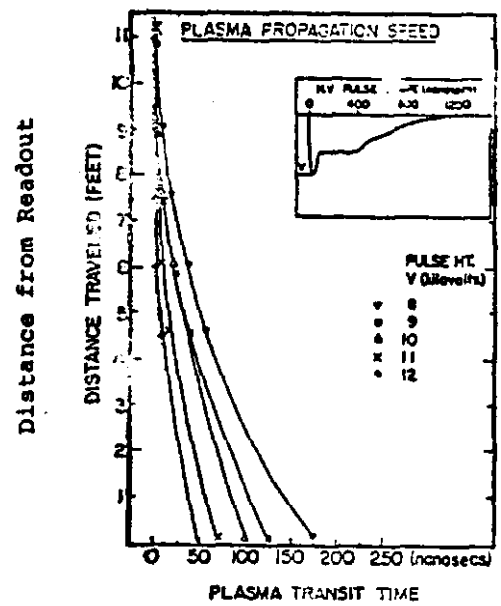

Fig. 2b Distance vs. time for actual HV pulse use on chambers.

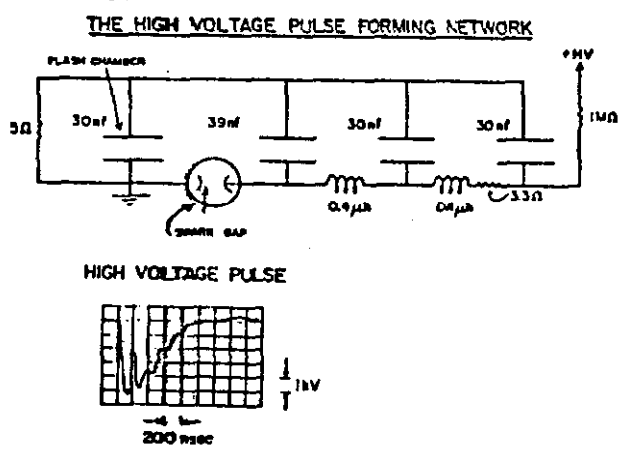

Fig. 3 The PFN circuit and a typical HV pulse.

The Read out System

The flash chambers are read out by using magnetostrictive wire techniques to detect the current pulse induced by the plasma discharge in a struck cell. The current pulse is induced on 0.118" (3 mm) wide copper strips roughly 20" (508 mm) long glued to the outside surface near the end of each polypropylene cell. These copper strips are connected to the chamber ground plane and form a set of capacitors (one for each polypropylene cell)with the chamber hot plane which acts as the other electrode. Each strip capacitor has the value of 3 picofarads. The plasma discharge, after propogating down the 12' long cell causes the capacitance formed between the copper readout strips and the hot electrode to change. This induces a roughly 0.5 A current pulse to flow through the copper strips to ground. The copper strips are made by photoetching copper clad mylar sheets with the appropriate cell-to-cell spacing. On the photoetched mylar, each strip is connected to a ground bus via a "sense" wire.

A 5 x 12 mil Remendur 27 magnetostrictive (m.s.) wire is layed over the sense wire region. The current pulse from a struck cell launches an acoustic pulse down the m.s. wire. The acoustic pulse propogates at roughly 5000 m/sec, corresponding to a 1 μsec separation for adjacent hit cells in the polypropylene. The chamber ground plane is made to lie over the photoetched strips insulated by a layer of 5 mm thick polypropylene. The polypropylene also reduces the shunt capacitance between the copper strips and the ground plane. Fig. 4 shows a schematic diagram of this construction.

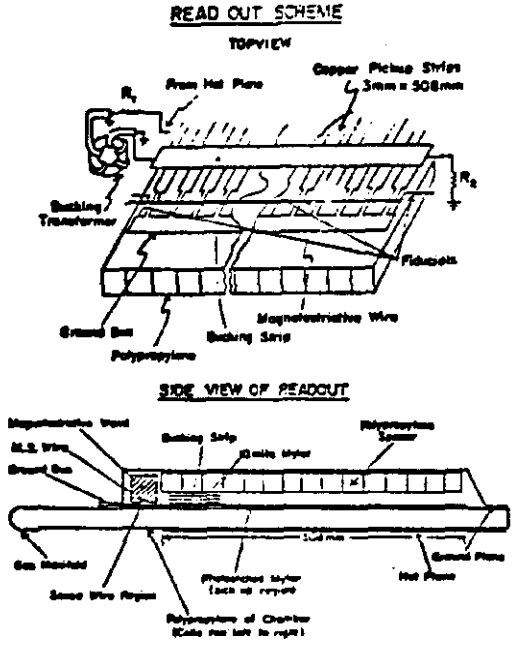

Fig. 4 Construction of the readout section.

With the chamber operating in the plateau region, this plasma induced current pulse is roughly 5 times larger than the current pulse induced on the copper strips when there is no plasma. To reduce the unwanted capacitance pickup when there is no plasma in a given cell, a type of A C bridge is made which balances the current through the sense wires. The bridge is produced by a 1:1 inverting cable transformer connected to the hot electrode of the chamber. The inverting transformer applies an opposite polarity pulse to a 2" wide aluminum "bucking strip" layed perpendicularly across all of the 0.118" copper strips. (See Fig. 4). The pulse on the bucking strip is optimized by resistance R_1 at its input and resistance R_2 at its output. This reduces the unwanted capacitive pickup by a factor of 3 to 4. Since the operation of the bucking circuit is determined by geometry, no individual tuning is necessary. In Fig. 5 are shown typical pulses from the magnetostrictive amplifier with the bucking turned off and turned on. A typical signal to background ratio of 10:1 to 20:1 is achieved when the bucking circuit is properly tuned.

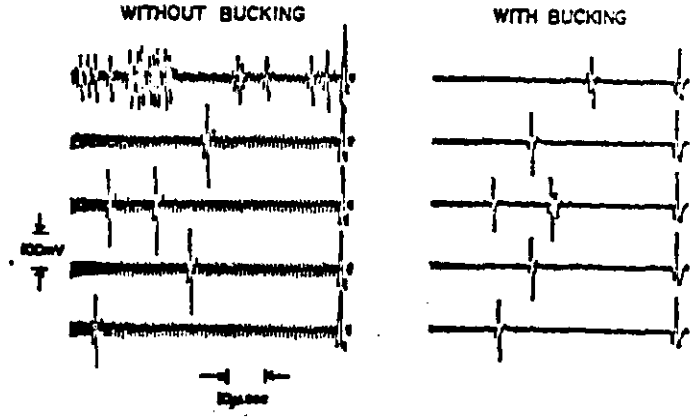

Fig. 5a Typical pulses from the wand amplifier without and with the bucking.

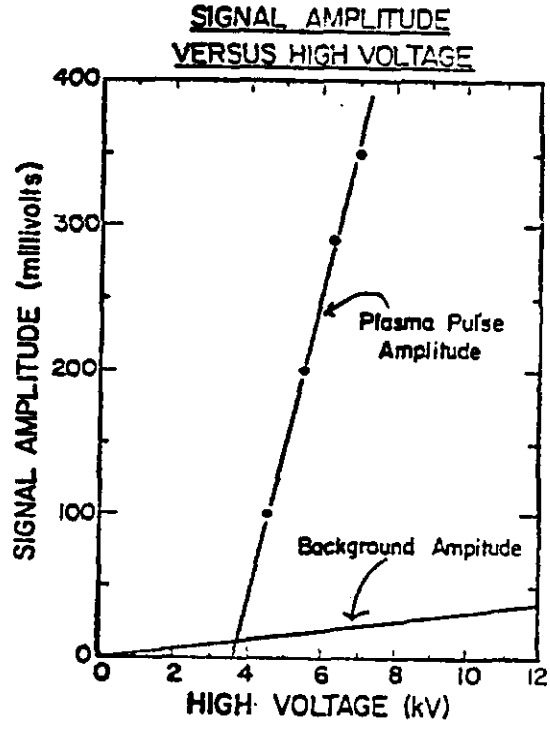

Fig. 5b The signal amplitude and the backgrounc amplitude vs. the high voltage.

The magnetostrictive wire is held in a 10 mil deep groove in a long extruded aluminum bar (wand). Teflon tape isolates the m.s. wire from the extruded aluminum bar and from the atmosphere. Dry N_2 is flowed in the teflon tape bag to prevent the m.s. wire from corroding. A solenoidal coil is wound around the entire length of the wand to periodically magnetize the m.s. wire. We found that there is an optimum magnetization of the m.s. wire which minimizes dispersion, and limits the attenuation of the acoustic pulses down 6' of wand to less than 20%.

Amplifiers with a gain of $\sim 10^3$ at each end of the wand provide the analogue signals for the readout system. Fig. 6 shows the wand construction.

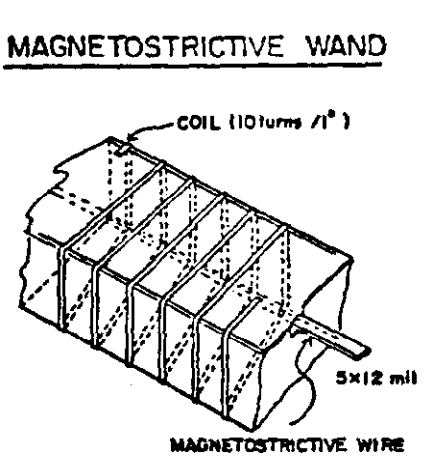

Fig. 6 The magnetostrictive wand construction.

Three fiducials, one at each end and one at the middle of the chamber calibrate the wand. Typical pulse amplitudes from the flash chamber are 100 to 200 mV. The use of two amplifiers per wand limits the number of cells to 366 which must be monitored per amplifier.

Tests have shown that the photoetched pattern readout region is less efficient that the rest of the chamber by the geometric factor of 0.118/0.20 ~ 0.60. Apparently the E field in the uncovered region between the copper strips is insufficient to efficiently start the plasma discharge. This inefficiency presents no problem since the readout section is placed outside of this 12' x 12' chamber sensitive area.

Each wand amplifier feeds a discriminator circuit which in turn clock signals into a 1024 x 1 memory. The discriminator threshold is programmed with an exponentially decreasing value to compensate for the 20% attenuation of signals from the middle fiducial regions. The clocking of the memory advances at a frequency such that $2+\epsilon$ (ϵ is a small number) counts occur per microsecond. Hence the 1024 x 1 memory allows slightly more than one half of the number of cells in a given flash chamber to be digitized by a given amplifier-discriminator-memory board. The use of this clock frequency avoids synchronization problems and ambiguities caused by slight variations in the cell separation.

The memory boards are read out by an asynchronous into CAMAC to a PDP-11 computer. Fig. 7 is a block diagram of the read out system.

Construction Cost

A flash chamber plane can be built by an unskilled labor crew of 5 at a rate of roughly 3 per 8-hour day. The cost of one flash chamber plane is roughly $400 parts and labor for the flash chamber plane, $100 for the wand and amplifiers and roughly $100 for the PFN high voltage pulsing system. We have set up a small factory and expect to finish the construction of the entire 600 flash chamber planes in about 7 months. To date we have produced roughly 200 completed flash chamber planes.

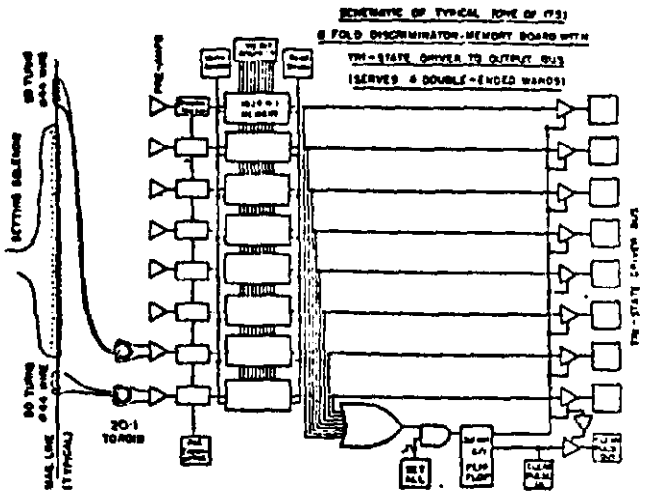

Fig. 7 Block diagram of the readout system.

Chamber Performance

We have tested 40 chambers with cosmic rays. Here we will describe the typical behavior of the 40 chambers. Typical data for these tests were taken from cosmic ray muon tracks through 16 chambers such as those shown in Fig. 8.

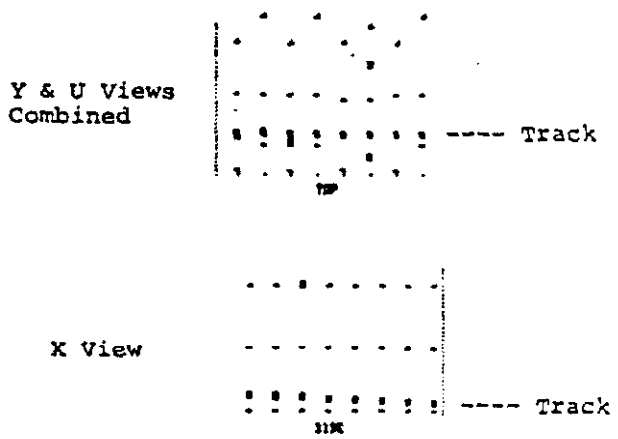

Fig. 8 Cosmic ray muon tracks through 16 chambers (1 module).

The high voltage characteristics for 4 chambers forming a U-X-Y-X unit are shown in Fig. 9. Potted in the same figure is the average multiplicity of hit cells per trigger. We see that from 3.75 kV to 5 kV all chambers follow the same curve and reach a plateau at an efficiency of 90%. Roughly half of the 10% inefficiency is due to the inner wall thickness which separates individual cells. The remaining 5% inefficiency is thought to be due to recombination of the initial ionization electrons and sweeping of these electrons by the HV pulse before the avalance mechanism begins. The multiplicity per trigger is a slowly increasing curve.

The uniformity of the high voltage response of a chamber has been tested by measuring the HV plateau of an X chamber at various locations. The results of this study show that the chamber is uniformally efficient over the entire 12' x 12' sensitive area at a high voltage $\geq$ 3.75 kV.

The operating range of the discriminator has been investigated. On the plateau, there is a discriminator level

range of roughly ±50%, where the chamber is efficient and where the average multiplicity and the percentage of adjacent double hits is well behaved. Fig. 10 shows a typical discriminator curve.

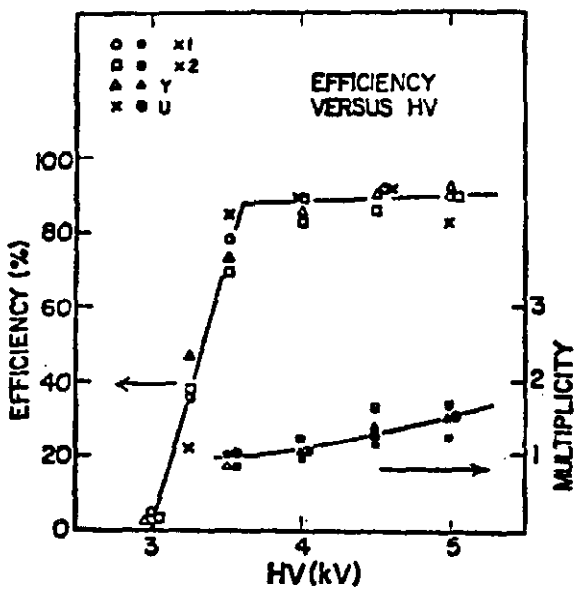

Fig. 9 Typical HV plateaus of 4 chambers forming a "beam".

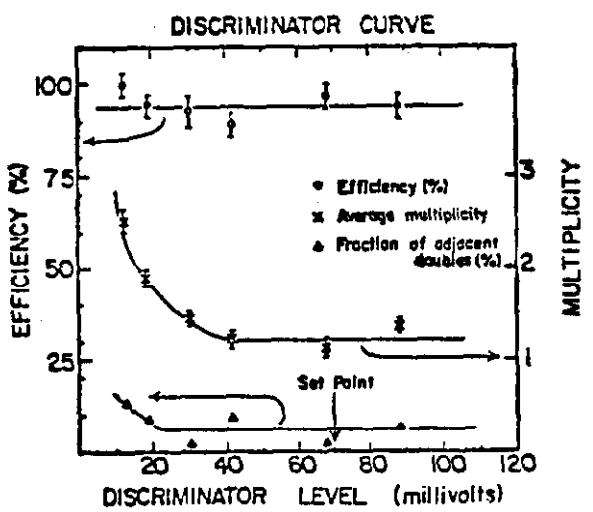

Fig. 10 Typical discriminator curve.

The chamber efficiency versus delay is shown in Fig. 11 for various gas flow rates. We see that the chamber sensitive time may be adjusted by varying the gas flow rate. Delays of roughly 600 nsec can be tolerated with a small loss of efficiency (9.6% at a rate of ~16%/ μsec) at a chamber gas flow of 1.5% vol./min. Higher gas flows can extend the efficient region to longer sensitive times.

The recovery time of the flash chambers has been investigated by refiring the high voltage pulse after a variable delay time and measuring the probability for the struck cells of the initial event to reignite. The recovery time measured as a reignition probability versus delay is shown in Fig. 12. We see that the flash chambers are limited to only 1 event every 2 seconds. This rate is adequate for measurements in the FNAL neutrino beam which is pulsed once every 10 seconds. A small electronegative gas impurity in the Ne-He chamber gas may shorten this recovery time, but care must be taken not to significantly shorten the chamber sensitivity time. (We have not yet studied the use of quenching agents in the gas.)

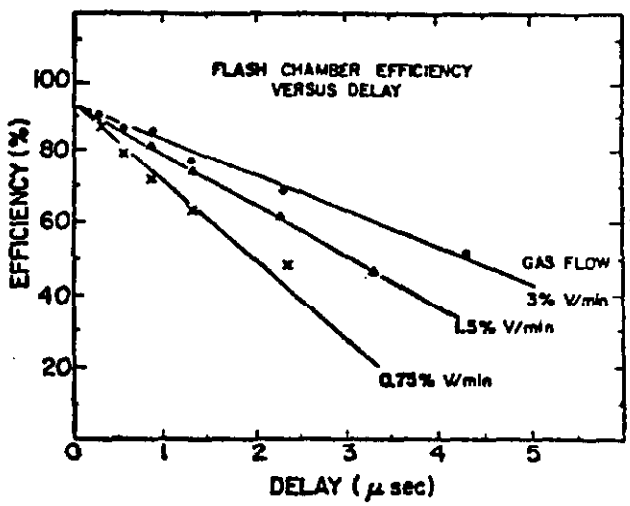

Fig. 11 The flash chamber efficiency versus delay for various flow rates.

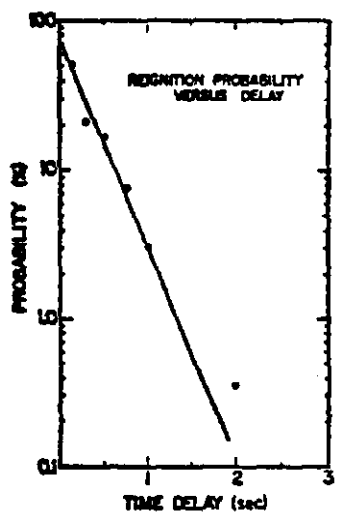

Fig. 12 The reignition probability versus delay.

The shower response of the flash chamber has been measured extensively in the test calorimeter and has been reported earlier.[2] Fig. 13 a and b show photographs taken of two typical electron showers and typical hadron showers in a 6 3 plane test calorimeter. The flash chambers in the test calorimeter were 17" x 17". We observe that the flash chambers are capable of supporting many tracks with no noticable degradation of efficiency. The high pattern recognition capability makes electromagnetic showers easily distinguishable from hadronic showers. We wish to varify that this excellent shower response is maintained in the full size flash chambers with the subsequently developed electronic readout.

A typical wand output for a cosmic ray shower is shown in Fig. 14. We see that the adjacent cells are easily separated. Fig. 15 is a computer reconstruction of the X view of a large shower in one module (16 chambers) of the calorimeter. Individual tracks are easily distinguished.

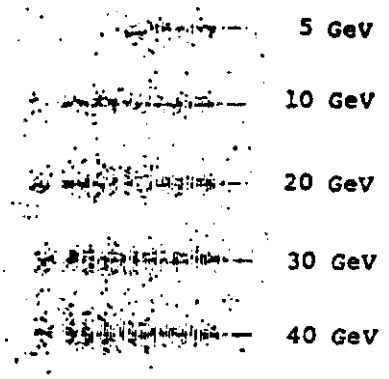

Fig. 13a Typical electron showers in the test calorimeter.

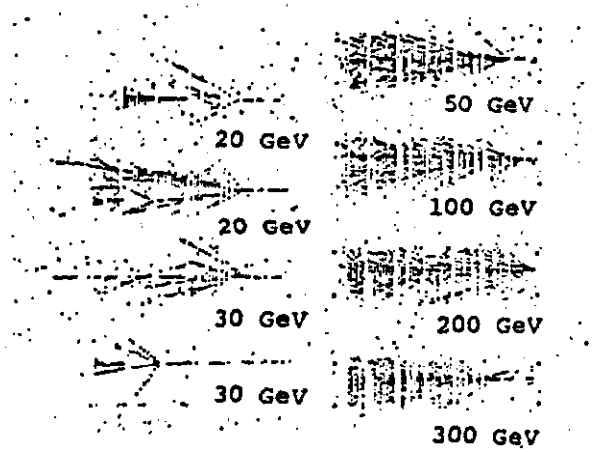

Fig. 13b Typical hadron showers in the test calorimeter.

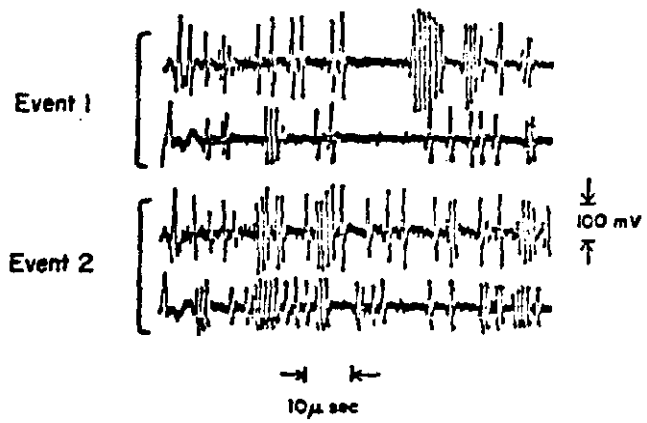

Fig. 14 The wand amplifier output for a massive shower.

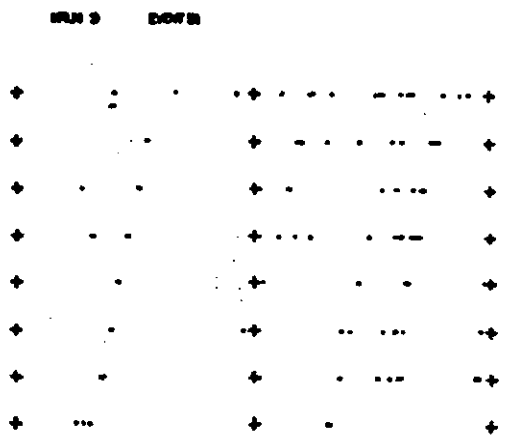

Fig. 15 Computer display of 8 X chambers responding to a large shower.

To measure the multitrack efficiency of the chambers, the output of one wand amplifier was fed simultaneously into 8 different discriminators. Fig. 16 shows the fraction of hit cells lost for a fixed discriminator setting versus the number of hit cells in one flash chamber plane. We see that up to 100 hits per plane may be read out without loss of efficiency. Higher multiplicity showers have a slowly decreasing efficiency and even for truely massive showers of 400 hits per plane, only 23% of the total number of hit cells are lost. A typical 200 GeV hadron shower will give no more than 60 hit cells at the shower maximum, and thus there is a large safety margin. The number of hit cells at the shower maximum is expected to rise slowly, so that even at 1 TeV where ~ 100 flash chamber cells are expected to be hit in the shower maximum, showers will be detected with a high efficiency.

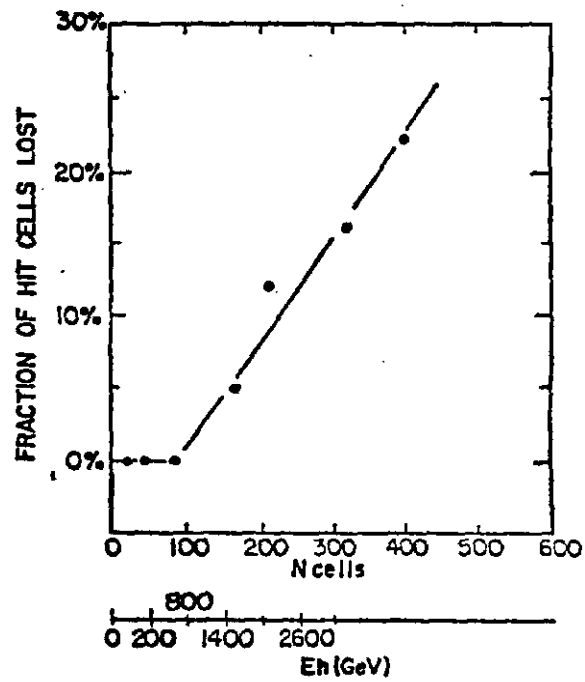

Fig. 16 The fraction of hit cells which are below a fixed discriminator setting versus the number of hit cells in the flash chamber plane.

Flash Chamber Calorimetry

The flash chamber is a digital device. Hence to obtain good energy and angle measurements, the flash chambers must be deployed with a fine granularity. The flash chambers can measure the energy flow direction of a shower and can determine the energy of the shower by counting the total number of cells which are hit. Furthermore, the patterns of the shower development can be used to distinguish hadronic from electromagnetic showers. Here we apply some additional higher energy measurements of the test calorimeter[2] to the calorimeter under construction in the FMMN experiment to predict the resulting energy and angular resolutions for electron and hadron showers.

Fig. 17 shows the overview of the calorimeter under construction. Roughly 340 metric tons can be constructed in the 60' space available. A set of 3 - 24' solid iron toroidal magnets and 4 - 12' toroidal magnets located downstream of the calorimeter momentum analyze muons. The sensitive area of the calorimeter is 12' x 12'.

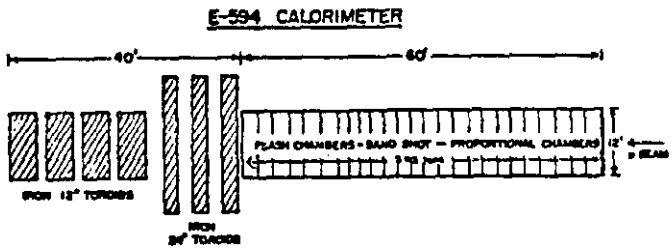

Fig. 17 The plan view of the FMMN calorimeter.

The construction of one module is shown in Fig. 18. The module is composed of 4 - 4" wide beams of 4 flash chambers each in the sequence U-X-Y-X. The flash chambers are placed between layers of 5/8" thick acrylic plastic extrusions filled alternatively with sand and with steel shot. Proportional tube planes are placed at the ends of the module to provide a trigger and an independent measure of the shower energy. Liquid scintillation counters are placed every 80 chambers (5 modules) to give a high efficiency fast timing signal.

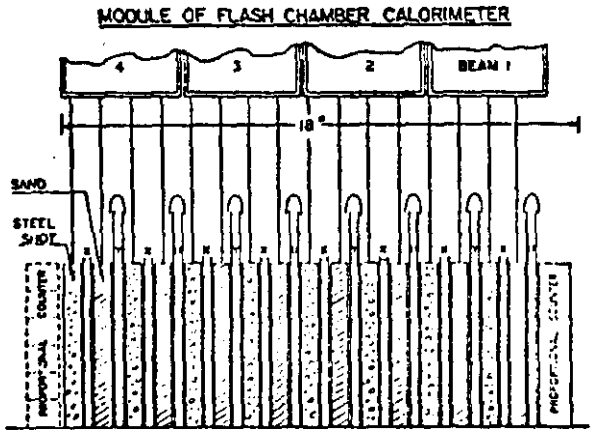

Fig. 18 The details of the construction of one module of the calorimeter.

The average sampling of the flash chambers per view is 7.2 g/cm^2, corresponding to 43.6% of a radiation length and 6.11% of an absorption length. The average distributed density of the calorimeter is 1.4 g/cm^3. The particular combination of 1 plane of sand with $\hat{\rho}_3$ = 1.45 g/cm^3 and 1 plane of steel shot with $\hat{\rho}$ = 3.10 g/cm^3 gives an average Z of 21. This construction is a good compromise for angular resolution, energy resolution, shower containment and neutrino event rate.

The expected angular resolutions for the FMMN calorimeter are shown in Fig. 19a and 19b for electron induced showers and for hadronic showers respectively. These data are taken from the test calorimeter and scaled to the FMMN calorimeter sampling step of 7.2 g/cm^2 per view. These resolutions are somewhat better than those reported by the CHARM collaboration[3] at CERN. Good angular resolution is of extreme importance in obtaining good resolution on the scaling variables for the semi-leptonic weak neutral current deep inelastic scattering experiment and for the background discrimination in the ν_μ elastic scattering experiment.

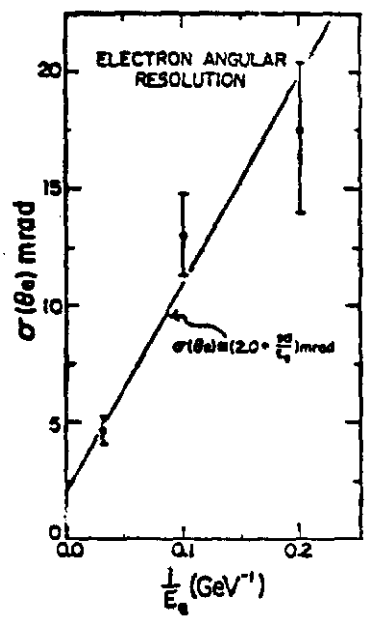

Fig. 19a The expected angular resolution of electron showers in the FMMN calorimeter.

The energy resolution of the calorimeter is determined by the fluctuation of the number of firing cells in a given shower, and the energy response curve of the calorimeter. All three flash chamber views may be used for the energy determination, hence the appropriate sampling step is 3.6 g/cm^2.

The electron energy resolution is shown in Fig. 20a. We see that the statistical fluctuations of the number of firing cells decreases as $E_e^{-\frac{1}{2}}$, but the nonlinear energy response arising from the firing of all the chamber cells in the shower core makes the resulting energy resolution roughly constant with energy. The estimated hadron energy resolution is shown in Fig. 20b. Substantial corrections for the leakage out the end of the test calorimeter had to be applied to make this estimate. Here the energy resolution at low energies improves with increasing energy until at high enough energies (~ 100 Gev) the nonlinear response starts to degrade the energy resolution.

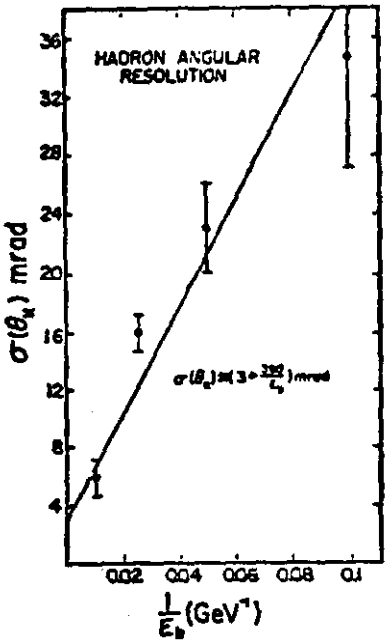

Fig. 19b The expected angular resolutions of hadron shower.

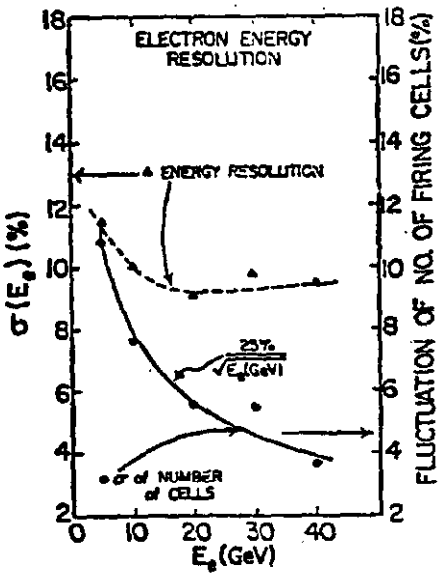

Fig. 20a The expected electron energy resolution.

Summary

The flash chamber is an inexpensive, simple device which is well suited for accelerator neutrino physics. We have demonstrated that the flash chamber has excellent multi track efficiency which is necessary for high energy hadronic cascade measurements. The electronic read out scheme we have developed permits the utilization of flash chambers in very large arrays. The low cost and simplicity of these flash chambers make it possible to build large calorimeters with very fine grained shower sampling. The high pattern recognition capability of the calorimeter should make it possible to explore new areas in neutrino physics at TeV energies.

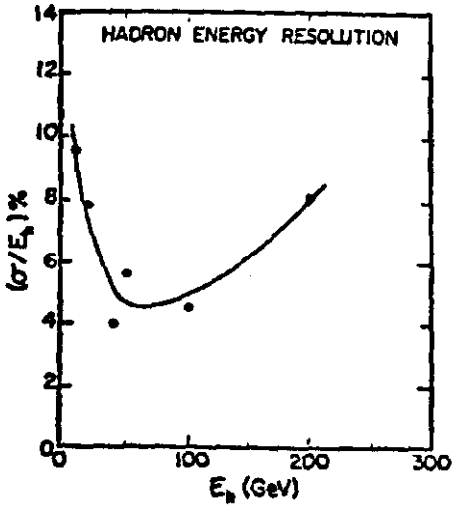

Fig. 20b The estimated hadron energy resolution.

Acknowledgments

The authors wish to thank M. Atac, S. Bristol, N. Bosek, D. Burandt, A. Cook, C. Kerns, R. Olsen, C. Lindenmeyer, S. Mori and R. Oudt for engineering and technical support. We also wish to thank the DOE and the NSF for support of this work. Special thanks to T. Ohsugi who helped on the early phase of this experiment.

References

[1] M. Conversi and L. Federici; NIM 151, 93 (1978)

[2] F. E. Taylor, et al.; IEEE NS-25, 312 (1978)

[3] Private Communication: K. Kozanecki, CHARM collaboration

*Permanent address: Northern Illinois University, DeKalb, Illinois.